*Journal of Microelectronics and Electronic Packaging* (2019) **16**, 103-116

ISSN: 1551-4897

# Flexible PET Substrate for High-Definition Printing of Polymer Thick-Film Conductive Pastes

Art Dobie*

*Abstract*—**A major obstacle in screen printing conductive low-temperature curing polymer thick-film (PTF) pastes onto common flexible PET substrate materials is the substantial spread of the pastes beyond the designed line width after printing. Industry observation and controlled testing have shown this spread can be as much as 80% over the circuit design's intended line width. This phenomenon prevents designers from increasing circuit density and/or reducing circuit real estate without incorporating other more involved and higher cost patterning methods. In many cases, flexible circuit fabricators, desiring more accurate high-definition circuit elements, may have to subcontract parts out of house to incorporate alternate patterning methods. This subcontracting, in turn, leads to a loss of control of both cost and lead time. This article will provide results of numerous in-house and field testings, comparing printed line width control, edge definition, and improved conductivity of printed polymer Ag conductors on different flexible PET substrates.**

*Keywords*—**PET substrate, fine line printing, acutance, higher conductivity**

## Introduction

A new screen emulsion stencil material exhibiting high image resolution characteristics was developed to provide improvements in printed accuracy and definition of high-end industrial and electronic screen printing applications. Whereas the response from the printed electronics industry related to this new screen stencil material was positive, user feedback identified that the intended precision was not achievable on flexible substrate materials currently used in the printed electronics industry. High accuracy and precise definitions of printed circuit elements provide the opportunity for increased density, reduction of circuit footprint, ability to finer feature sizes, reduced paste consumption, and even better conductivity. However, regardless of the accuracy and clarity of a circuit image reproduced in a printing screen's stencil component, the accuracy of the resulting printed image significantly degrades as the printed paste noticeably spreads on the surface of the flexible substrates commonly used in the printed electronics industry. This recognition has led to the development and testing of a new advanced flexible polyester (PET) substrate-level solution for improving the accuracy of screen-printed circuit elements.

The manuscript was received on February 15, 2019; accepted on April 11, 2019

The original version of this paper was presented at the 51st Symposium on Microelectronics (IMAPS'2018) in Pasadena, CA, October 9-11, 2018.

Chromaline/Ikonics, 4832 Grand Avenue, Duluth, Minnesota 55807

*Corresponding author; email: adobie@chromaline.com

## Screen Printing Process

Screen printing is the most commonly used method of paste deposition for creating circuit elements such as conductive traces, dielectric layers, and resistors. In the screen printing process, an open weave mesh is stretched and elongated to a specific level of tension and secured to a stable framework. A water-soluble, photo-imageable stencil coating is normally applied to the underside of the tensioned screen mesh. This coating is then imaged with the desired print design using opaque masking (typically in the form of a photopositive film) and UV light in the 300-400 nm spectral range. As the UV light passes through the nonopaque areas of the masking, it cross-links the photosensitive emulsion coating, rendering it water tolerable. The areas of the design which represent the desired print areas are opaque on the photomask. These opaque areas block the UV light from striking the photosensitive coating, preventing these sections from cross-linking and keeping them water soluble. A water spray development process is then applied to the exposed screen and the areas of the stencil coating, which were masked from the UV light and remained water soluble to then eventually dissolve and rinse away, creating openings in the stencil coating in the geometries of the print features.

The imaged printing screen is normally secured to either a printing machine or a printing fixture. The substrate is placed immediately below the screen, typically on a vacuum stage that is X, Y, and Theta adjustable for registration purposes. The screen is mounted directly over the substrate nest and elevated a specific distance (gap) above the substrate surface. This gap distance is approximately equal to 1/200th of the inside dimension of the screen frame.

This gap, termed the screen "off-contact" distance, is one of the crucial factors of the screen printing setup. Screen printing and metal stencil printing are the only contact printing processes requiring ink or paste to move completely through the printing plate (the screen or metal stencil), from the far side down through the imaged pattern openings and out the opposing side nearest to the substrate surface. Printing with a metal stencil can be successfully accomplished with the stencil directly in contact with the substrate surface. However, in screen printing, the presence of the mesh filaments in a screen creates a substantial surface area within the imaged pattern openings. The mesh surface area competes with the substrate surface for adhesion of the printing ink. When screen printing is attempted in an on-contact mode, some of the paste remains with the screen mesh and does not completely transfer from the screen to the substrate.

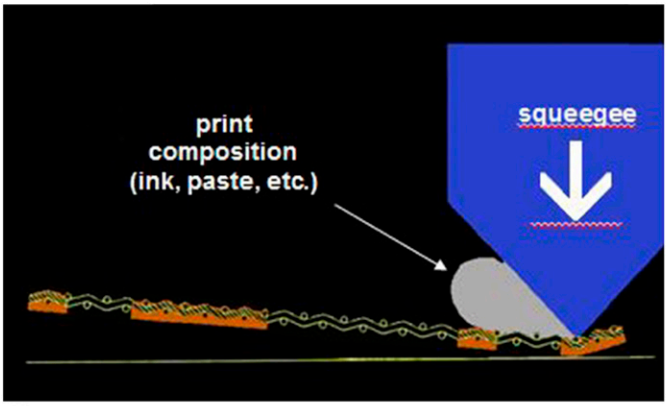


(a)

Fig. 1A. Paste transfer via the off-contact screen printing process.

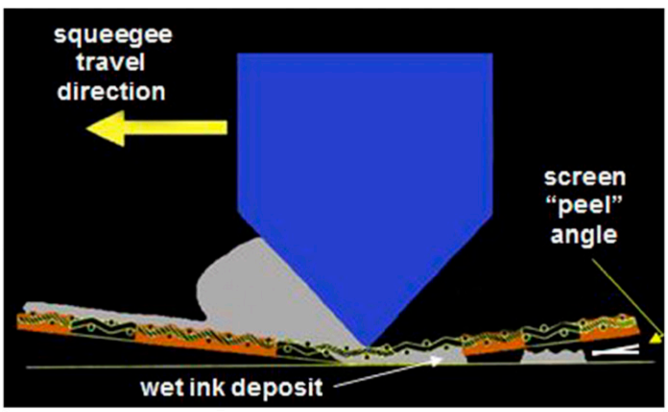


(b)

Fig. 1B. Paste transfer via the off-contact screen printing process.

This often leaves voids or peaks in a partial ink deposit. Incomplete ink transfer in the on-contact print method is the main reason for the "off-contact" distance requirement in the screen printing setup. In an off-contact printing setup, the squeegee pushes down and deflects the screen in a single line of contact against the substrate surface. The squeegee then begins to travel laterally, forcing ink into the imaged pattern openings in the screen. The screen mesh tension combines with the off-contact gap to create enough counterforce behind the moving squeegee to pull the screen mesh up and out of the ink deposit left behind on the substrate (Figs. 1a and 1b).

## Thick-Film Paste Technology

Conductive inks or pastes formulated for electronic applications are a suspension of a functional phase (conductive particles), a binder, vehicle, and perhaps other additives. The binder is used to create adhesion between the printed ink and the substrate. The vehicle component is typically an organic composition of resins and solvents (and any required modifiers) which gives the ink printability. Although many precious and noble metals are used in electronic materials, silver is the most

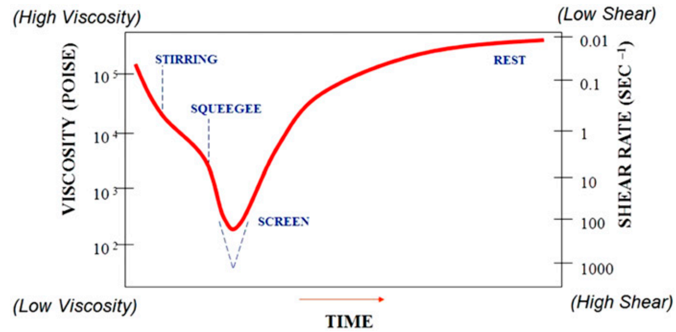


Fig. 2. Pseudoplastic rheology: Behavior of ink viscosity during printing.

common conductive component in inks used for low-temperature curing of polymer thick-film materials. Most of these materials incorporate flake morphology; in some cases, monospherical powders, or a mix of flake and powder is also used. The size and volume of the solids in the paste are a major factor when selecting a screen mesh to print that paste.

These pastes exhibit specific behavior when subject to an applied shear stress, such as stirring, or squeegeeing during the screen printing process. Viscosity is often defined as a fluid's resistance to flow and is measured under controlled and standardized conditions. Viscosity of materials tends to be significantly affected by certain variables, such as temperature. Rheology can be defined as the flow of matter under the influence of an applied stress. In the case of printing inks and pastes, rheology is used to describe the behavior of ink viscosity during printing. When considering printing inks or pastes, viscosity is more a snapshot of a specific moment, where rheology could be considered a home movie of an ink's behavior during printing over a specific window of time.

Most printing inks are formulated to be "pseudoplastic," or shear thinning, where the viscosity decreases as the shear rate increases. This is beneficial to screen printing, as these types of pastes decrease in viscosity and become more fluid once the squeegee begins to shear the ink during the print stroke. The more fluid paste can flow more freely as it travels into and out of the open mesh cells in the patterned areas of the screen during printing.

The formulation of these shear thinning materials also have a "recovery" side to their rheological curve (Fig. 2), causing the paste to quickly return to its original "rest" viscosity once the shear stress being applied to the paste is ceased. This recovery part of the rheological curve prevents the paste from continuing to flow, creating the ability to retain some level of print definition rather than an undefined mass of ink. The length of the recovery time of a given paste can help the printed paste level out and prevent mesh marks and other imperfections on its surface. However, although helpful to achieve a smoother printed surface, slower recovery time can also lead to increased ink spread. The wide range of viscosity recovery times of different PTF paste formations can increase the amount of ink spread over that which normally occurs on common flexible PET substrates.

## Experimental Method

Testing of the newly developed screen emulsion stencil and advanced flexible PET substrate materials designed to improve

Table I
Screen Mesh Types Used in PE Applications

| Mesh type | Mesh count | Thread diameter | Mesh opening | Mesh thickness | Open area | Mesh WIFT | Suggested minimum line width |
|---|---|---|---|---|---|---|---|
| SS | 290 | 20 | 68 | 45 | 60% | 27 | 75 |
| PET | 305 | 33 | 47 | 50 | 32% | 16 | 150 |
| SS | 325 | 28 | 50 | 59 | 41% | 24 | 150 |
| SS CAL | 325 | 23 | 54 | 48 | 50% | 24 | 100 |
| Polyarylate | 330 | 23 | 54 | 43 | 49% | 21 | 100 |
| PET | 355 | 35 | 31 | 55 | 19% | 10 | 180 |
| SS | 360 | 16 | 55 | 36 | 60% | 22 | 40 |
| SS CAL | 360 | 16 | 55 | 32 | 60% | 19 | 40 |
| PET | 380 | 30 | 33 | 45 | 24% | 11 | 180 |
| SS | 400 | 18 | 46 | 39 | 51% | 20 | 50 |
| SS CAL | 400 | 18 | 45 | 29 | 51% | 15 | 50 |
| PET | 420 | 27 | 30 | 40 | 25% | 10 | 180 |
| SS CAL | 500 | 18 | 32 | 29 | 41% | 12 | 40 |
| SS | 590 | 15 | 30 | 30 | 49% | 15 | 35 |
| SS CAL | 640 | 15 | 25 | 21 | 40% | 8 | 30 |
| SS CAL | 730 | 13 | 22 | 18 | 40% | 7 | 20 |

the accuracy of screen-printed circuit elements was performed both in-house and in the field. Considering that both of these new materials were formulated to improve printed image accuracy, all print testings were performed using both materials simultaneously. The testing involved criteria such as image size reproduction accuracy, edge definition, and resolution for the new screen emulsion, and accuracy, definition, resolution, printed profile, and line resistance of conductive traces printed onto the new PET substrate.

## Screen Technology

A printing screen was needed to perform the print tests. This required the selection of an appropriate mesh type before fabricating the screen. The criteria for mesh selection include the following:

1. Minimum artwork size requirements (smallest line or space size)
2. Desired wet ink film thickness (WIFT)
3. Ink/mesh relationship (Can the proposed ink pass through the chosen mesh without clogging?)
4. Screen cost (capability versus dollars)

To aid in the mesh selection process, Table I displays mesh types used in the printed electronics industry.

Because of its higher strength, stainless steel mesh typically has smaller wire diameters than polyester mesh having similar mesh counts. This is identified in the "open area" percentage column in Table I, and visually apparent in Figs. 3a and 3b which display a 50% open area stainless steel mesh compared with a 25% open PET mesh.

When mesh counts are similar, the mesh with larger thread diameters will exhibit smaller openings with a more closed porosity (open area). The particle size in most low-temperature Ag PTF pastes is typically between 1 and 4 μm, with the solid content between 60% and 90%. The higher open area and larger mesh openings of the 400 stainless steel wire mesh offer less obstruction to paste flow than a polyester mesh of similar thread count per inch. The smaller diameter of the 400-18–μm wire mesh permits smaller artwork sizes to be imaged into the screen

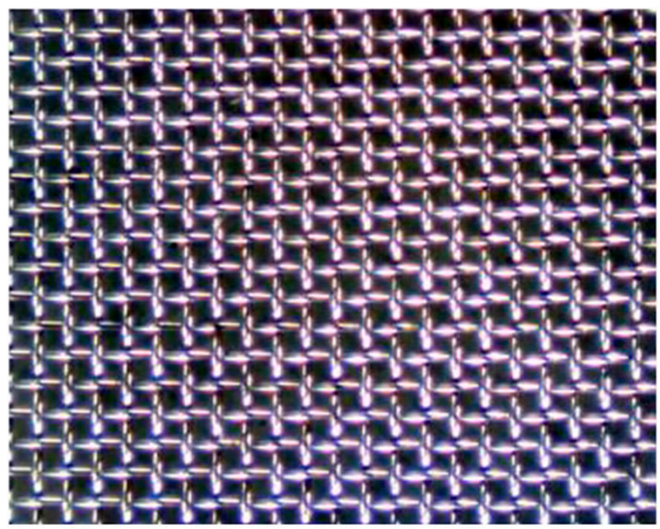

(a)

Fig. 3A. High open stainless steel wire mesh.

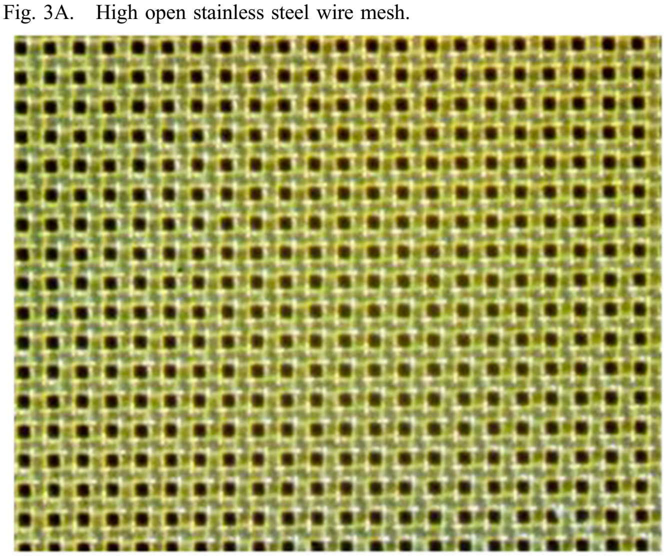

(b)

Fig. 3B. Lower open polyester mesh.

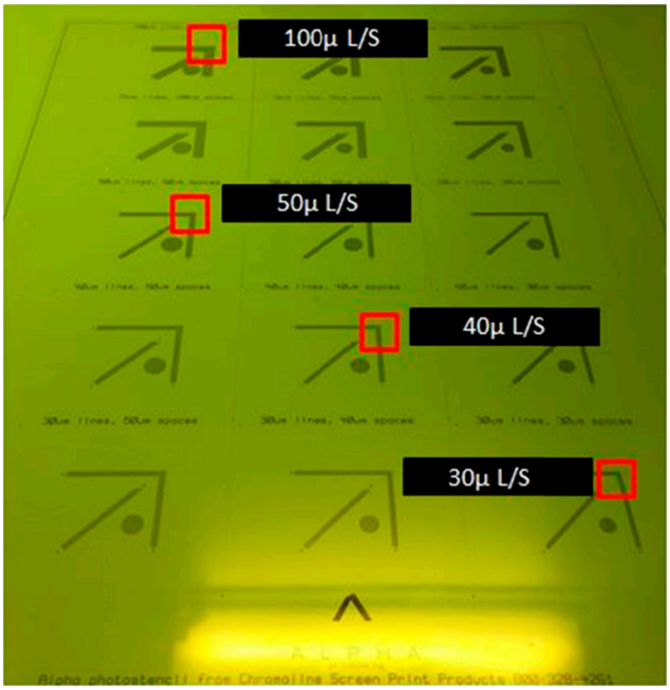


Fig. 4. Measurement areas of screen stencil imaged with print test pattern.

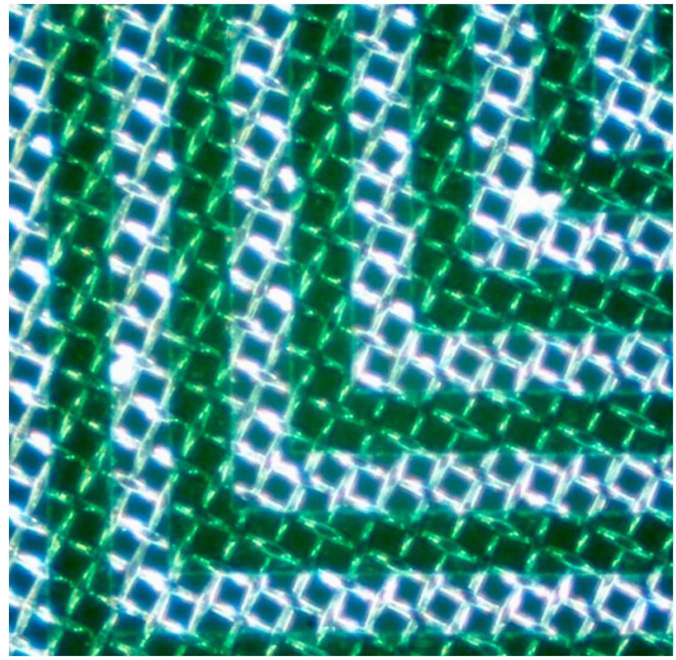

Fig. 5. 100-μm image in the test screen.

Table II
Sizes of the cured 100-μm line widths printed on the three different test substrates.

| Description | Substrate A | Substrate B | Substrate F |
|---|---|---|---|
| Target line width | 100 μm | 100 μm | 100 μm |
| Minimum line width | 164 μm | 136 μm | 96 μm |
| Maximum line width | 189 μm | 148 μm | 109 μm |
| Average line width | 178.5 μm | 142.7 μm | 101.4 μm |
| Average paste spread over target width | +79% | +43% | +2% |

stencil compared with the 420 count polyester. Although all of the stainless steel mesh types finer than the 400-18–μm mesh are also capable of printing the finest features on the test artwork (30 μm), they are substantially more expensive, rendering them somewhat cost prohibitive when larger area screens are required.

The screen emulsion component must also be capable of photographically reproducing the finest features of the intended print design. The newly developed stencil material was formulated with high-resolution capability and is able to resolve the minimum test artwork features (30 μm) with great accuracy. A 25-μm capillary film version of the new stencil material was selected for use on the 400-18–μm screen mesh as it provides an 8- to 10-μm emulsion over mesh thickness to aid in a suitable printed WIFT. It also provides a smooth screen surface to achieve a sufficiently gasket-like seal to the substrate surface to restrict ink bleed.

## Test Pattern

A test pattern was designed to evaluate the desired criteria of both the new screen emulsion and the new coated PET substrate. The test artwork incorporated lines and spaces, right

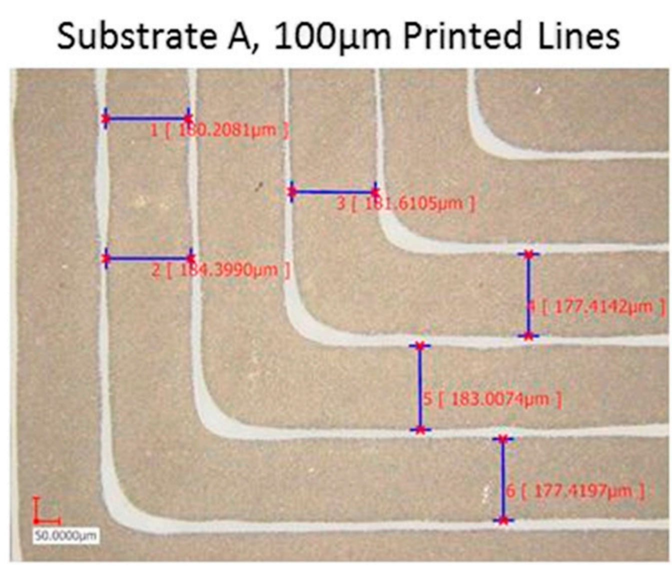


Fig. 6. Cured 100-μm L/s printed on substrate A.

angles, concentric circles, and biased lines and spaces arranged in rows and columns. Line sizes ranged from 100 to 30 μm, and the spacing between the lines varied as lines got narrower (Fig. 4).

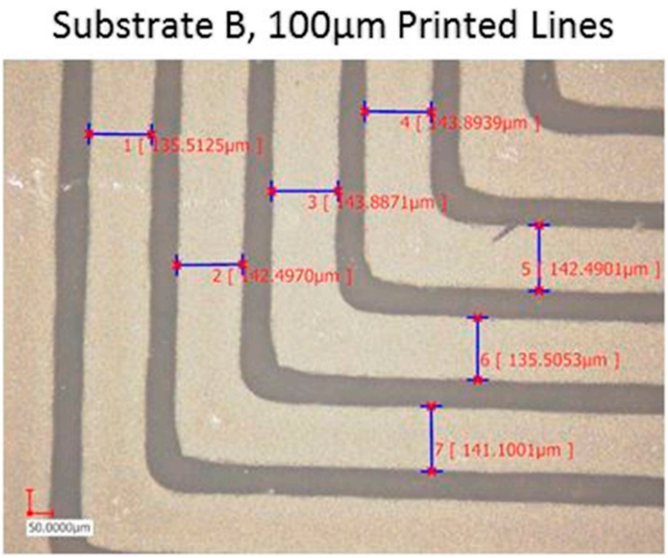


Fig. 7. Cured 100-μm L/s printed on substrate B.

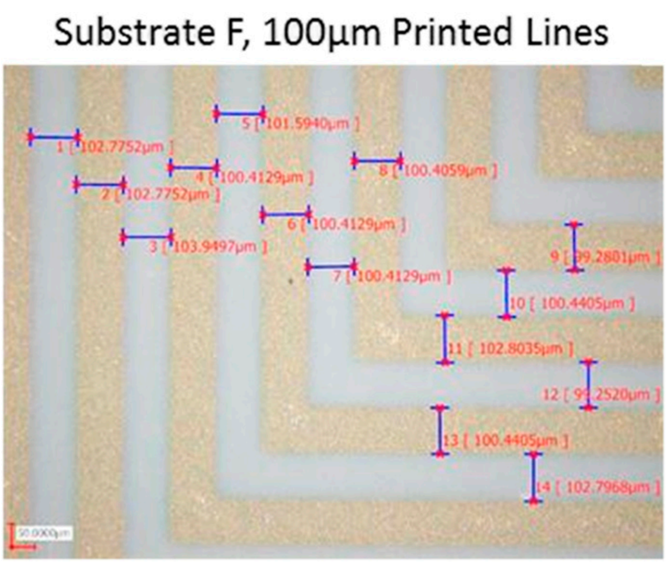


Fig. 8. Cured 100-μm L/s printed on substrate F.

The photomask used to image the test screen was a photo-positive film, photo-plotted at 30,000 ppi from a production CAD file. The line widths on the photo-plotted test positive were within 1 μm of designed sizes in the CAD file. Following screen exposure, the sizes of the images in the screen stencil were typically within 1 μm of the size of the corresponding feature on the photo-plotted film positive.

## Substrates Tested

Three different types of flexible PET substrates were included in the print testing:

1. Substrate A (common industry material): print-treated PET, with a primer for ink adhesion, prestabilized, and optically clear
2. Substrate B (also a common industry material): PET, surface treated for ink adhesion and high surface tension, prestabilized, hazy/translucent
3. Substrate F (newly developed): coated PET, with ink adhesion promoter and ink spread inhibitor, prestabilized, hazy/translucent

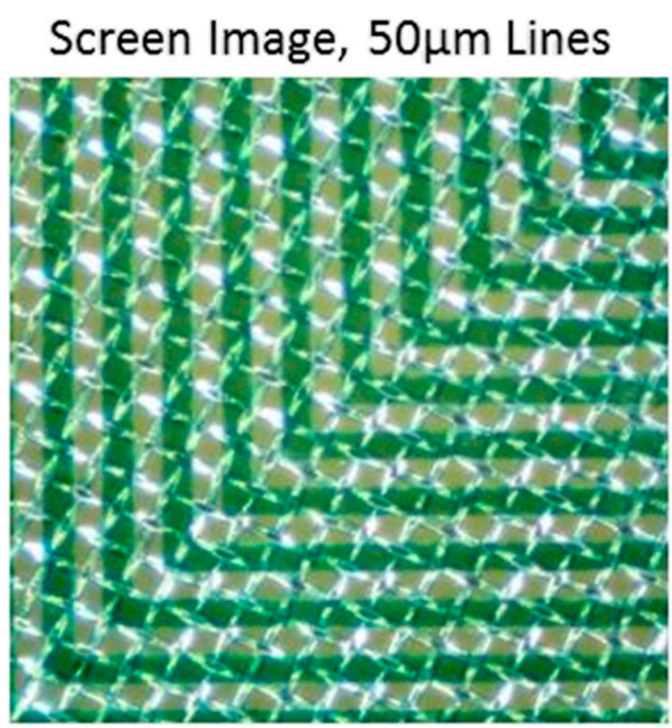


Fig. 9. 50-μm image in the test screen.

Table III
Sizes of the cured 50-μm line widths printed on the three different test substrates.

| Description | Target line width | Minimum line width | Maximum line width | Average line width | Average paste spread over target width |
|---|---|---|---|---|---|
| Substrate A | 50 μm | Unmeasurable | Unmeasurable | Unmeasurable | Unmeasurable |
| Substrate B | 50 μm | Unmeasurable | Unmeasurable | Unmeasurable | Unmeasurable |
| Substrate F | 50 μm | 44 μm | 54 μm | 49.1 μm | −2% |

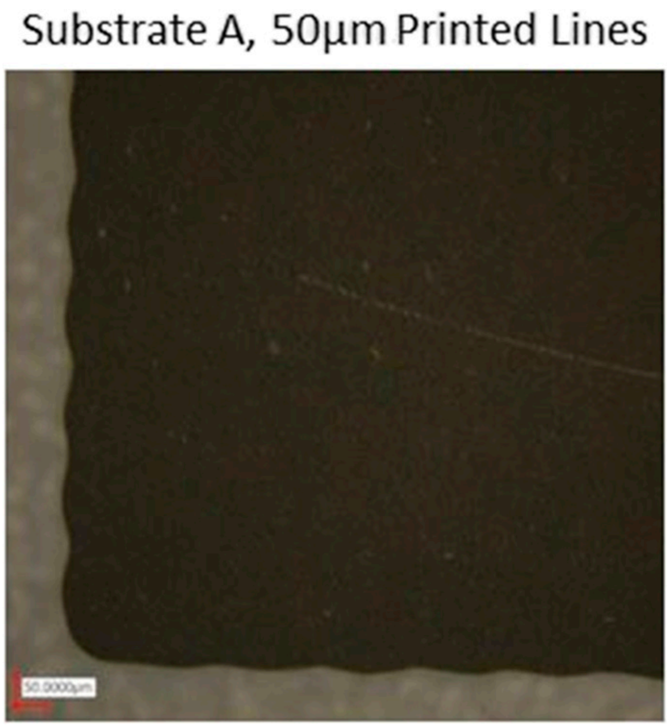


Fig. 10. Cured 50-µm L/s printed on substrate A.

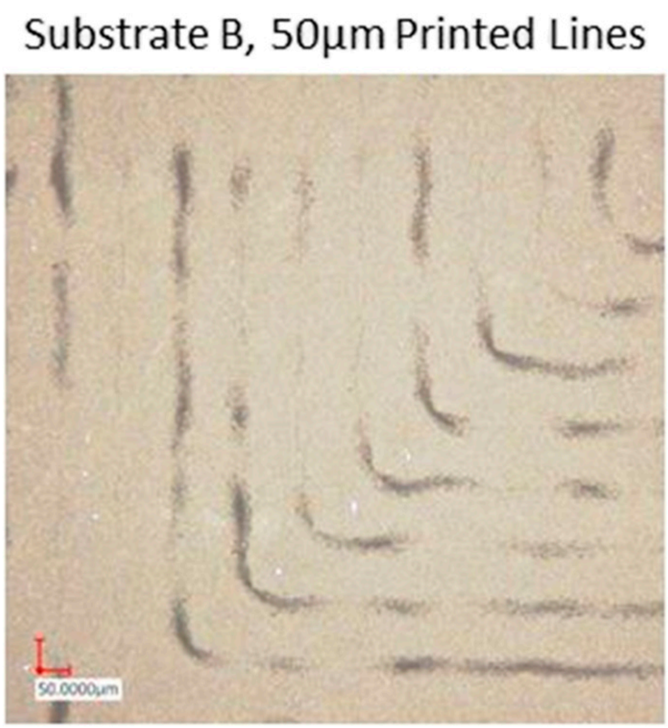


Fig. 11. Cured 50-µm L/s printed on substrate B.

## Print Testing

Screen print testing was conducted at various stages using different silver-loaded PTF conductor pastes. In all cases to date, "flat bed" screen printing was used, and all of these systems

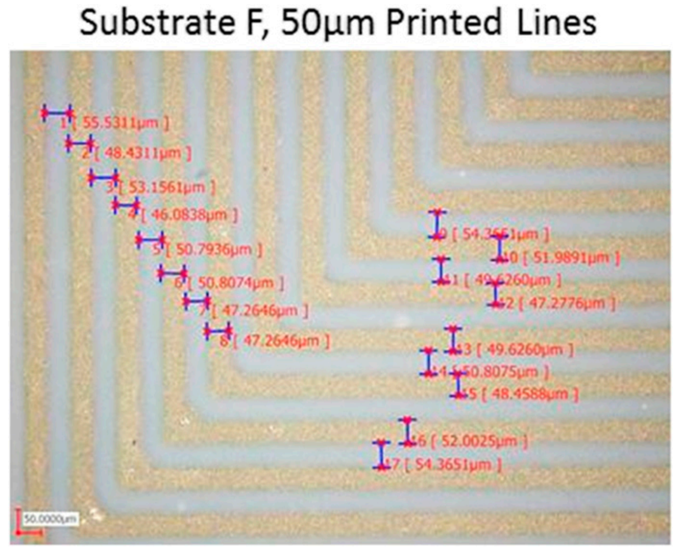


Fig. 12. Cured 50-µm L/s printed on substrate F.

were sheet-fed substrate insertion printing systems. The sheet-fed substrate placement method was advantageous for this testing as it allows for staging separate stacks of as many different substrates as needed for comparison and permits inserting them into the printing machine in any consecutive yet unbiased sequence.

Printer setup parameters used were as follows:

1. Flood stroke: 500 mm/s @ 20 kg pressure
2. Print stroke: 400 mm/s @ 30 kg pressure
3. Off-contact distance: 5.5-6.0 mm
4. Squeegee: 75/95/75 Shore A scale durometer, 10° attack angle, 16″ length w/factory edge

Common characteristics of the PTF pastes used in testing were silver conductor paste, viscosity of 10,000-13,000 cps, and shear thinning rheology, with a fine Ag flake morphology typically less than 4 µm in size.

## Print Test Results

The print test results show that the newly developed substrate "F" provides printed feature sizes that accurately reproduce the size of the corresponding images in the print screen. This result is consistent throughout the different line widths used on the test artwork. The high printed accuracy is due to the newly developed coating applied to the surface of substrate F. The same lines and spaces were printed on substrates A and B using the same screen and paste display substantial line spread. Table II displays the sizes of the cured 100-µm line widths printed on the three different test substrates.

The 100-µm line and space images in the test screen are presented in Fig. 5 for reference. Photos of the corresponding cured print results for the 100-µm lines and spaces appear in Figs. 6-8.

In the randomly selected areas measured for the cured 100-µm lines and spaces, ink spread on substrates A and B averaged between 43% and 79% over the target line width of 100 µm. Because of the properties of the coated surface of substrate F, the

Table IV
Sizes of the cured 40-μm line widths printed on the three different test substrates.

| Description | Target line width | Minimum line width | Maximum line width | Average line width | Average paste spread over target width |
|---|---|---|---|---|---|
| Substrate A | 40 μm | Unmeasurable | Unmeasurable | Unmeasurable | Unmeasurable |
| Substrate B | 40 μm | Unmeasurable | Unmeasurable | Unmeasurable | Unmeasurable |
| Substrate F | 40 μm | 34 μm | 46 μm | 40.9 μm | +2% |

Table V
Sizes of the cured 30-μm line widths printed on the three different test substrates.

| Description | Target line width | Minimum line width | Maximum line width | Average line width | Average paste spread over target width |
|---|---|---|---|---|---|
| Substrate A | 30 μm | Unmeasurable | Unmeasurable | Unmeasurable | Unmeasurable |
| Substrate B | 30 μm | Unmeasurable | Unmeasurable | Unmeasurable | Unmeasurable |
| Substrate F | 30 μm | 26 μm | 37 μm | 30.8 μm | +3% |

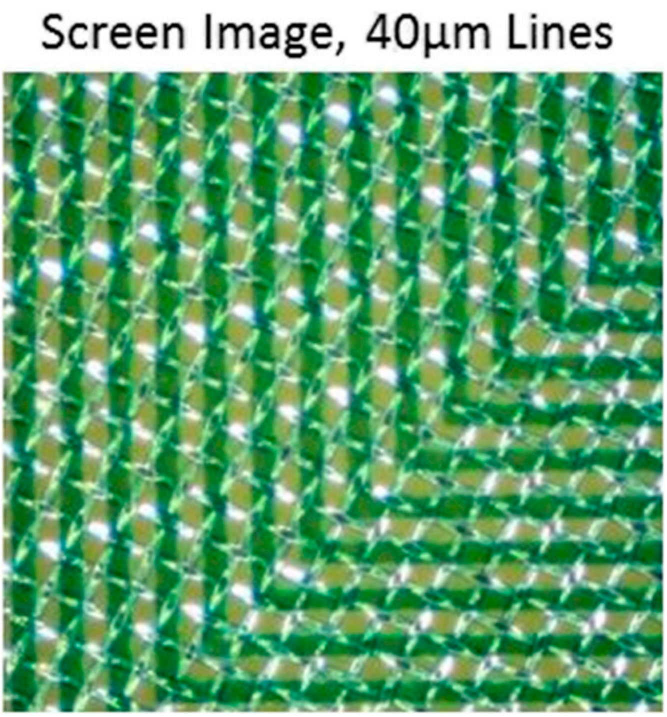


Fig. 13. 40-μm image in the test screen.

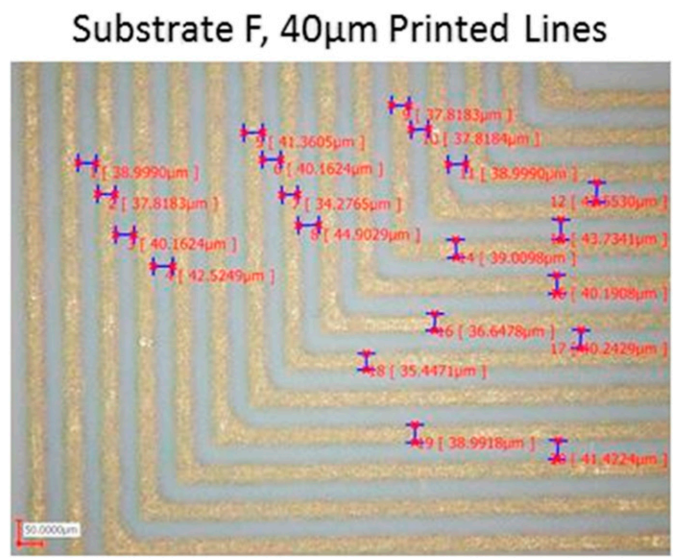


Fig. 14. Cured 40-μm L/s printed on substrate F.

paste spread on substrate F was measured to be no greater than 9%, with an average of just 2% at the same measured locations.

Print test results for the 50-μm line and space sections showed similar results, with the spread on substrates A and B being so significant that the paste actually migrated far enough that it overcame the pitch distance and shorted adjacent lines. In some cases, the paste flowed into a common mass similar, rendering them unmeasurable.

Table III displays the sizes of the cured 50-μm line widths printed on the three different test substrates. Line widths on substrates A and B were undeterminable due to substantial paste spread. The cured lines on substrate F remained within an average of 2% of the target 50-μm line width. Fig. 9 displays the 50-μm lines in the test screen stencil. Figs. 10-12 display the cured 50-μm line and space sections on the three tested substrates.

Test print results for the 40- and 30-μm sections on substrates A and B exhibited paste spread too significant to permit measurements. The 40- and 30-μm size prints on substrate F were well defined and exhibited an average of less than 4% paste spread (Tables IV and V).

Fig. 13 displays the 40-μm lines in the test screen stencil. Fig. 14 displays the 40-μm line and space measurements of the cured paste on substrate F. The printed and cured 40-μm lines were on average less than 3% of the target line size in the test design.

Fig. 15 displays the 30-μm lines in the test screen stencil. Fig. 16 displays the 30-μm line and space measurements of the cured paste on substrate F. The printed and cured 30-μm lines were on average less than 4% spread over the target line size in the test design.

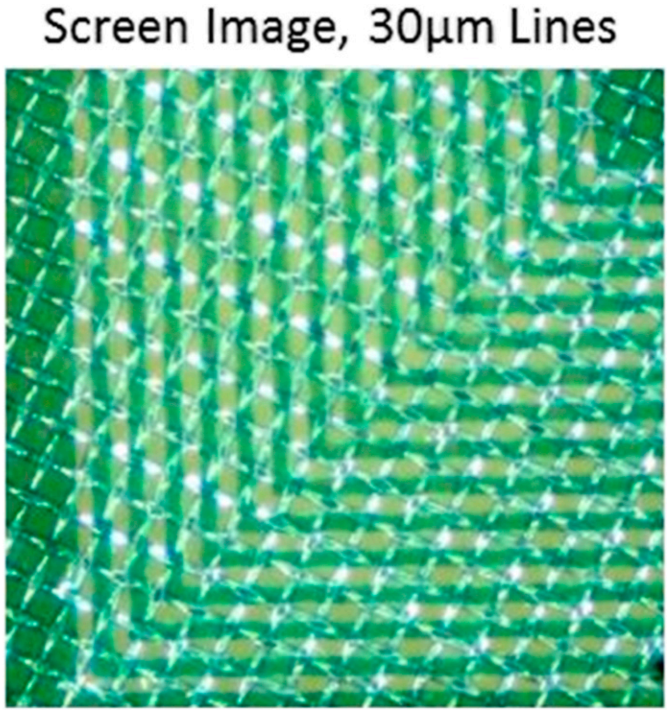


Fig. 15. 30-$\mu$m image in the test screen.

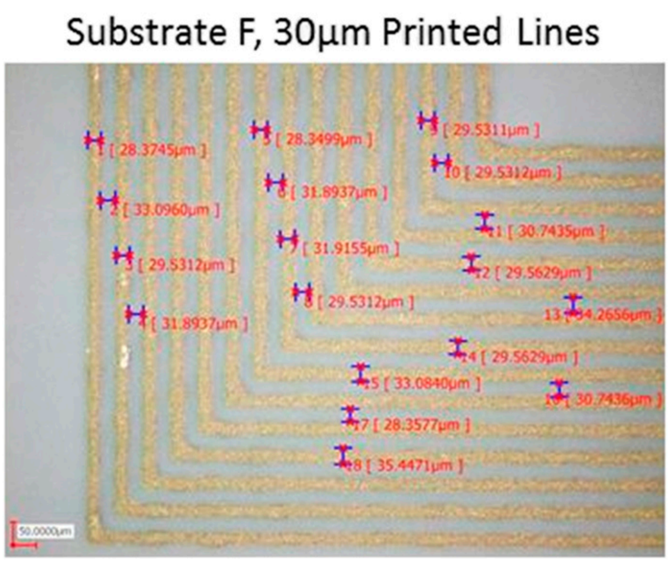


Fig. 16. Cured 30-$\mu$m L/s printed on substrate F.

It is theorized that the accuracy of the higher resolution image sizes (50, 40, and 30 $\mu$m) imaged into the newly formulated screen emulsion and, in turn, screen printed onto the newly developed substrate F is a byproduct of the increased resolution and ink spread retention characteristics designed into the performance of both materials [1].

Fig. 17 displays a comparison of concentric circles with 40 $\mu$m lines and spaces and 30 $\mu$m lines with 50 $\mu$m spaces printed onto substrates A and F with the same paste through the

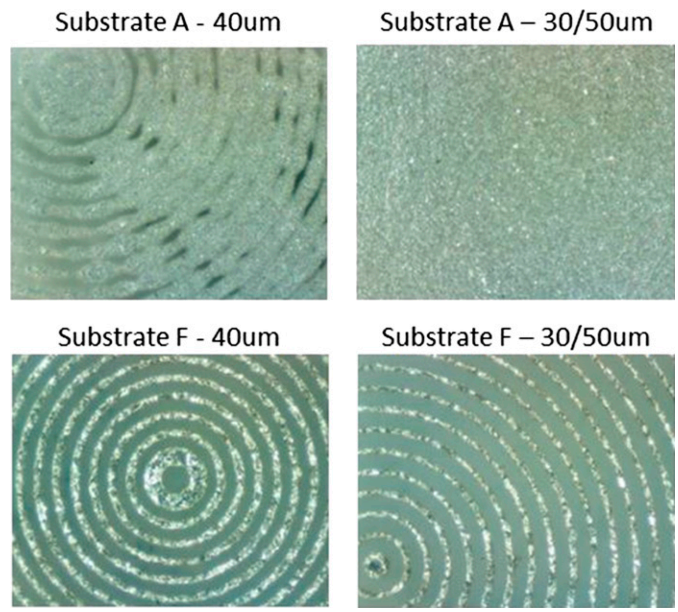


Fig. 17. Comparison of screen-printed high-resolution concentric circles on substrates A and F.

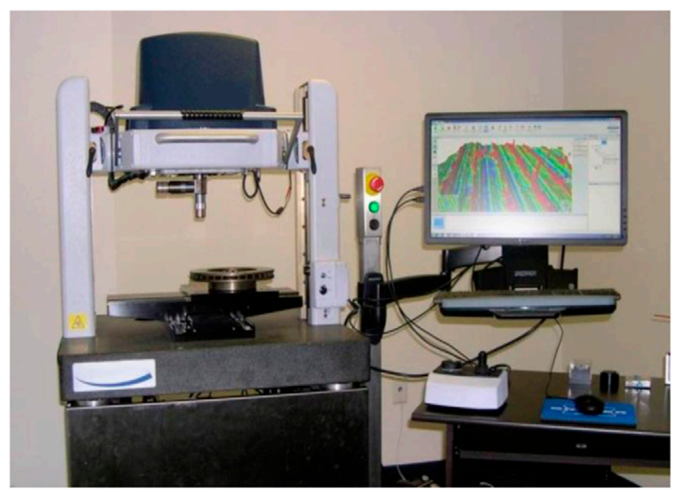

Fig. 18. Production 3D optical microscope.

same test screen using consecutive print strokes. Substrate B did not display discernable lines and spaces in the concentric circle areas.

## 3D Printed Profile Data

The printed silver traces were reviewed using a Bruker 3D optical microscope (Fig. 18) to capture profile data.

The significant spread on substrates A and B prevented capturing clean profile images, as depicted in Figs. 19 and 20.

Fig. 21 displays the 3D microscope data for silver traces printed on substrate F. Note the distinctly defined profile displayed in the "Y Profile" graph within Fig. 21.

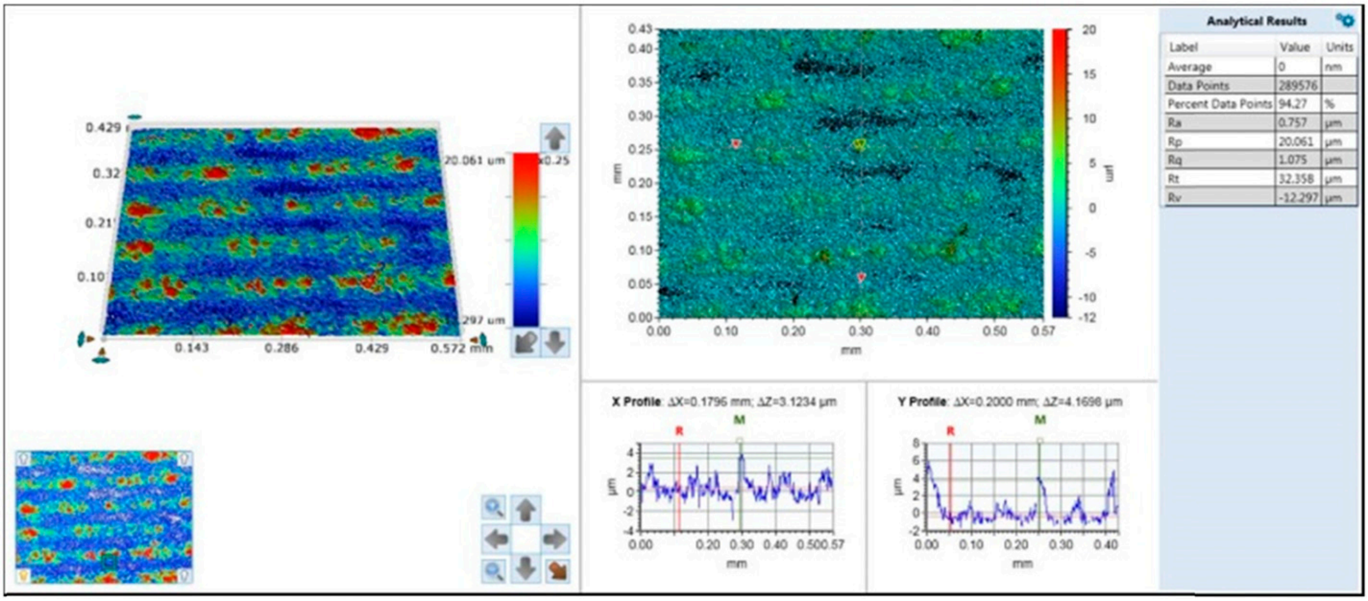


Fig. 19. 3D microscope data of 40-µm lines and spaces printed on substrate A.

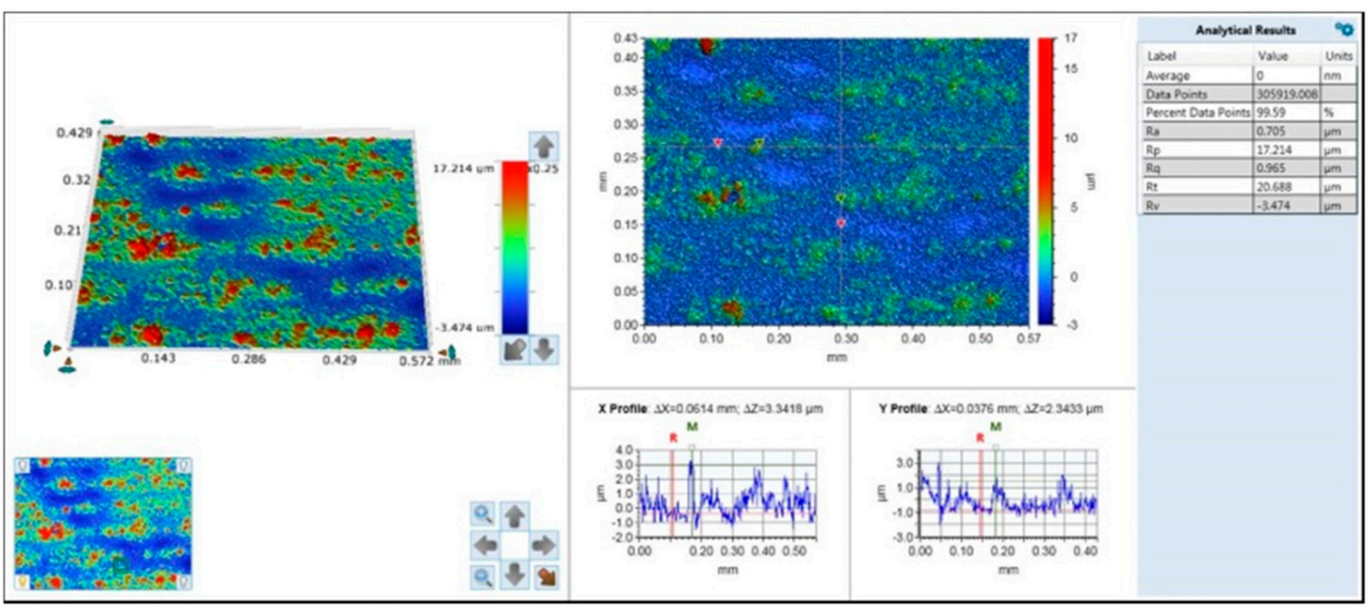


Fig. 20. 3D microscope data of 40-µm lines and spaces printed on substrate B.

The production 3D optical microscope was also used to capture 3D images of the 100- and 50-µm lines printed on substrate F and provide additional profile and thickness data (Figs. 22 and 23).

The cured 100-µm lines on substrate F were typically 10 µm in height, whereas the cured 50-µm-wide lines were typically 8 µm in thickness.

Screen print testing of 1000-µm-wide lines of a copper-based conductive paste was performed, and the printed profile and line width data are shown in Fig. 24. The printed copper conductive paste retained a desirable printed profile on substrate F compared with substrate A.

The more desirable profile of the printed copper is recognized as a result of the coated substrate F's paste "drawn in" and restriction of lateral paste flow.

## Resistance Measurements

Line resistance and volume resistivity were measured on both substrates A and F. (Substrate B's poor reproduction of the finer

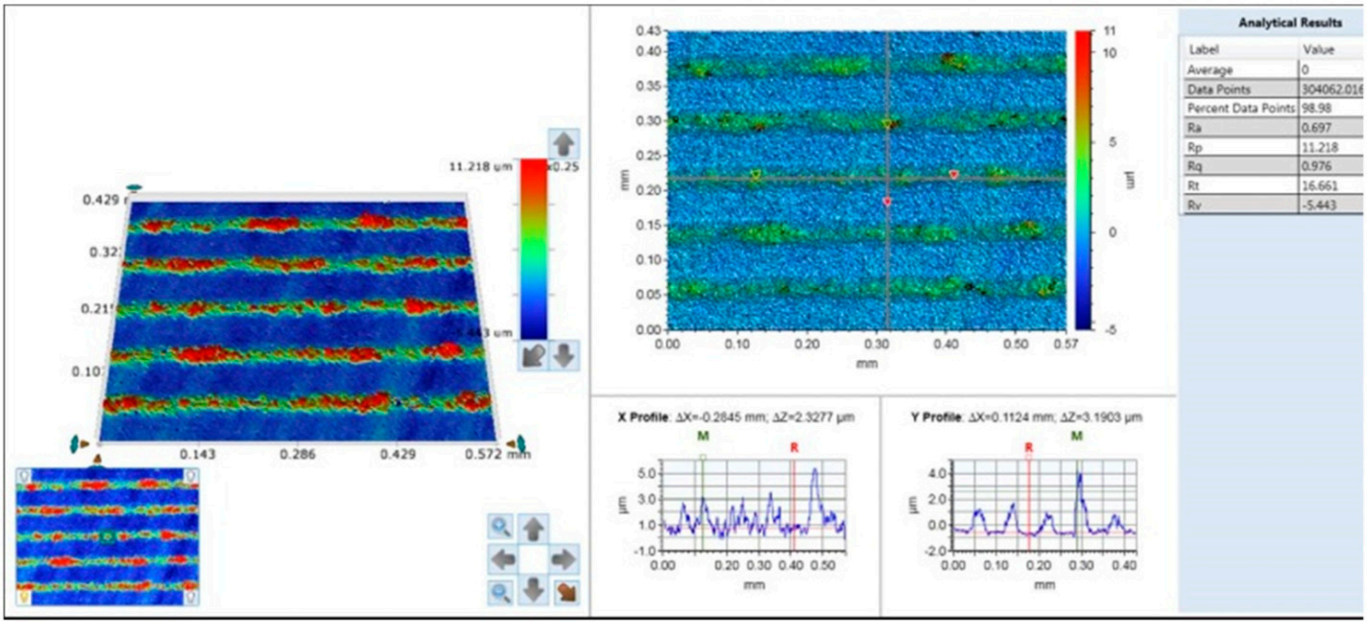

Fig. 21. 3D microscope data of 40-μm lines and spaces printed on substrate F.

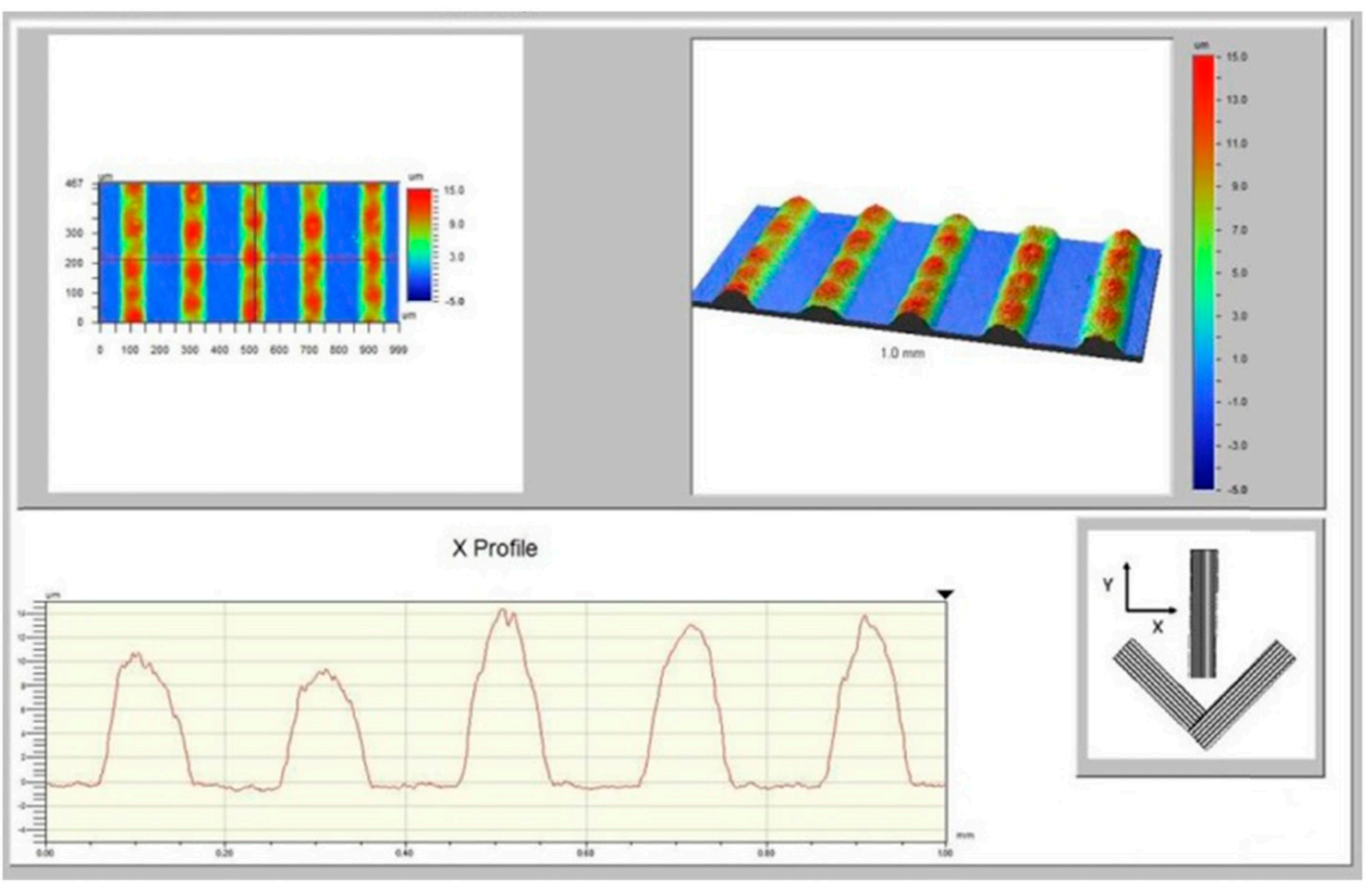


Fig. 22. 3D microscope data of cured profile and height of 100-μm lines on substrate F.

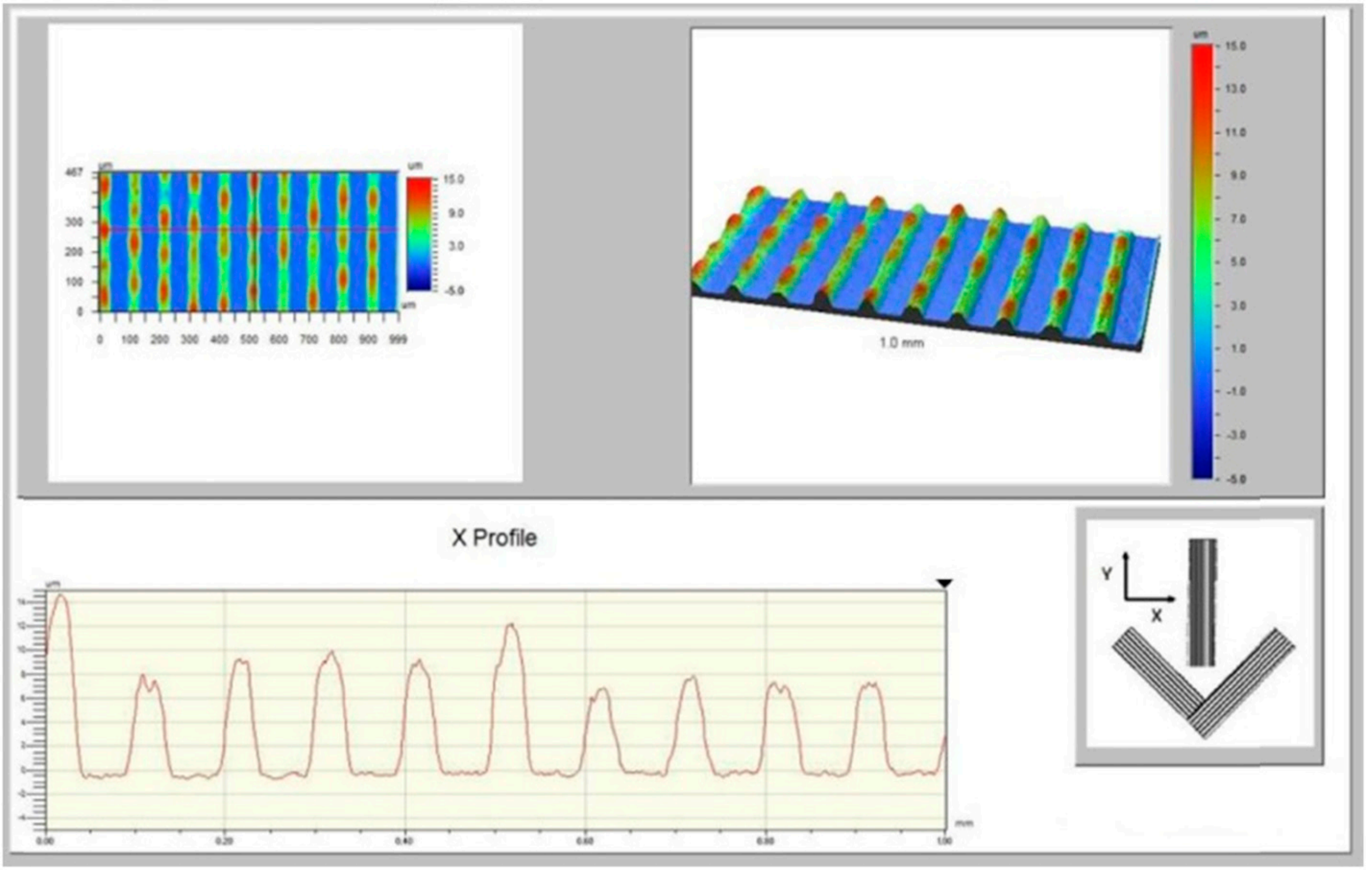


Fig. 23. 3D microscope data of cured profile and height of 50-μm lines on substrate F.

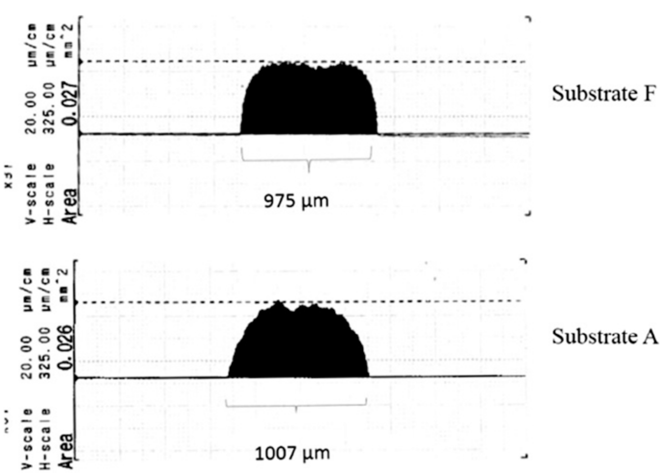


Fig. 24. Printed copper profile measurements [4].

line widths resulted in shorts and was not included the remaining measurement data.)

Additional data such as cross-sectional area, and the height and width of the cured traces were also monitored for comparison and their relationship to line resistivity.

Experience suggests that traces printed moments apart with the same paste reservoir through the same screen should have

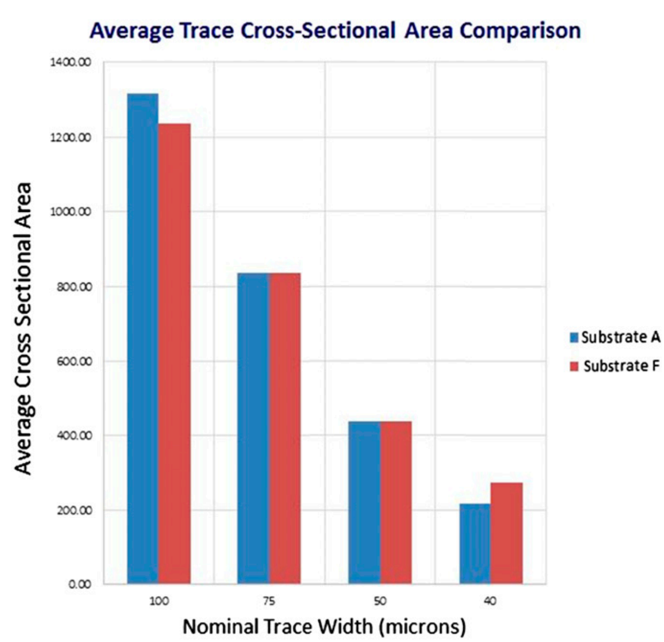


Fig. 25. Average trace cross-sectional area is relatively identical on substrates A and F.

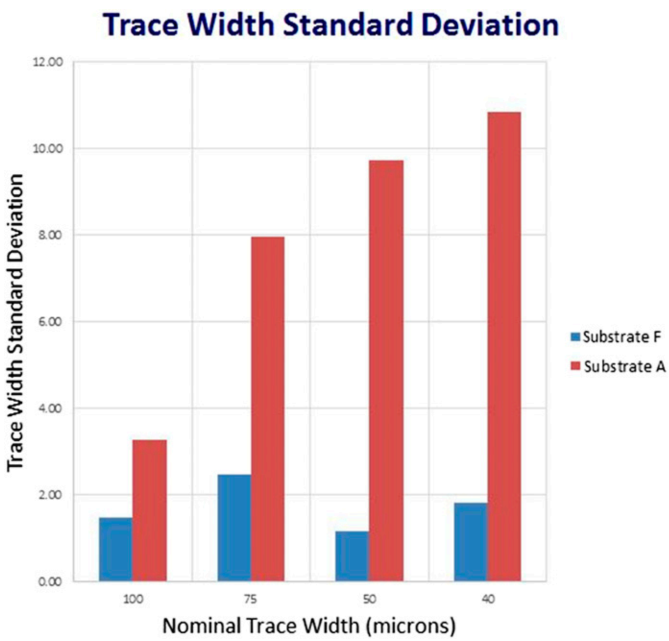


Fig. 26. Standard deviation of printed trace widths on substrates A and F.

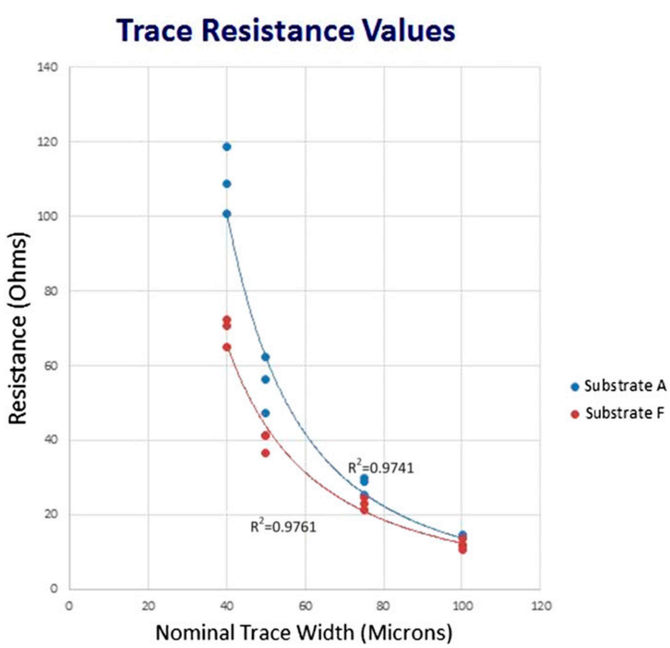


Fig. 27. Line resistance measurements on substrates A and F.

relatively identical deposition volumes. The Bruker 3D microscope was used to calculate the cross-sectional area of the cured Ag traces on both substrates A and F to confirm this industry recognized perception. Fig. 25 confirms that the consecutively printed silver traces on substrates A and F have similar cross-sectional areas, suggesting the volume of paste consecutively deposited on both substrates was very similar.

However, as shown in Tables II–V, the paste spread of the printed trace widths was significantly greater on substrate A than substrate F. Trace width measurements from the Bruker 3D microscope confirm that the standard deviation of those wider trace widths on substrate A was significantly greater than that of the more accurate trace widths measured on substrate F. This is illustrated in Fig. 26.

Resistivity was measured for the cured traces on both substrates A and F. This is displayed in Fig. 27.

Fig. 27 shows that line resistance values were consistently higher on substrate A than on substrate F, but that the delta in the line resistance measurements between substrates A and F decreases as the trace width becomes wider.

Volume resistivity data for both substrates A and F appear in Fig. 28 [1].

Fig. 28 shows that volume resistivity is lower on substrate F regardless of line width. Volume resistivity values for substrate A were 14-45% greater than those of substrate F.

Fig. 25 indicates that the same volume of the same paste was printed through the same screen onto both substrates A and F. Based on these data, the resistance values of identically cured, relatively equal volumes of the same paste would initially be expected to be very close, if not equal.

The data in Fig. 26 confirm that substrate A shows a significantly higher standard deviation in trace width than substrate F. Standard deviation for substrate F remained relatively constant, regardless of line width. The higher standard deviation of paste spread on substrate A suggests not only that the printed line widths on substrate A are greater in width than corresponding lines printed on substrate F, but also that the amount of line spread varies significantly. The smaller variation in line widths on substrate F for all line sizes tested permits more efficient use of the same amount of printed paste.

A hypothesis for understanding the lower resistance values measured on substrate F is that the reduced spread of the printed paste confines the conductive particles in narrower, more consistent wire-like lines, rather than permitting them to spread with the increased line widths. In addition, as the vehicle and solvents in the paste are drawn into the coating on substrate F, it is theorized that this activity also creates a tighter "packing" of the conductive particles, leading to better conductivity for the same deposited volume of the same paste [2]. Fig. 29 illustrates this concept of a more confined, tighter packing of the conductive particles in paste printed on substrate F than less efficient particle packing on substrate A or B (Fig. 30).

## Summary and Conclusions

Printed electronic circuit designs continue to move toward a tighter line pitch and reduced line widths as a means to increase functional density and reduce overall circuit area. Feedback from printed electronics manufacturers suggests that the biggest inhibitor to greater accuracy of printed circuit elements is the standard flexible substrate materials currently used in printed electronics fabrication. Recognition of these factors led to the development of a new flexible PET substrate and high-accuracy screen stencil material, specifically designed to reproduce printed image sizes with an increased degree of accuracy. Although improvements to screen printing presses, squeegees, screen mesh, and conductive paste technology have evolved in recent years, the concept of a substrate-level solution to improve printed accuracy is much less common.

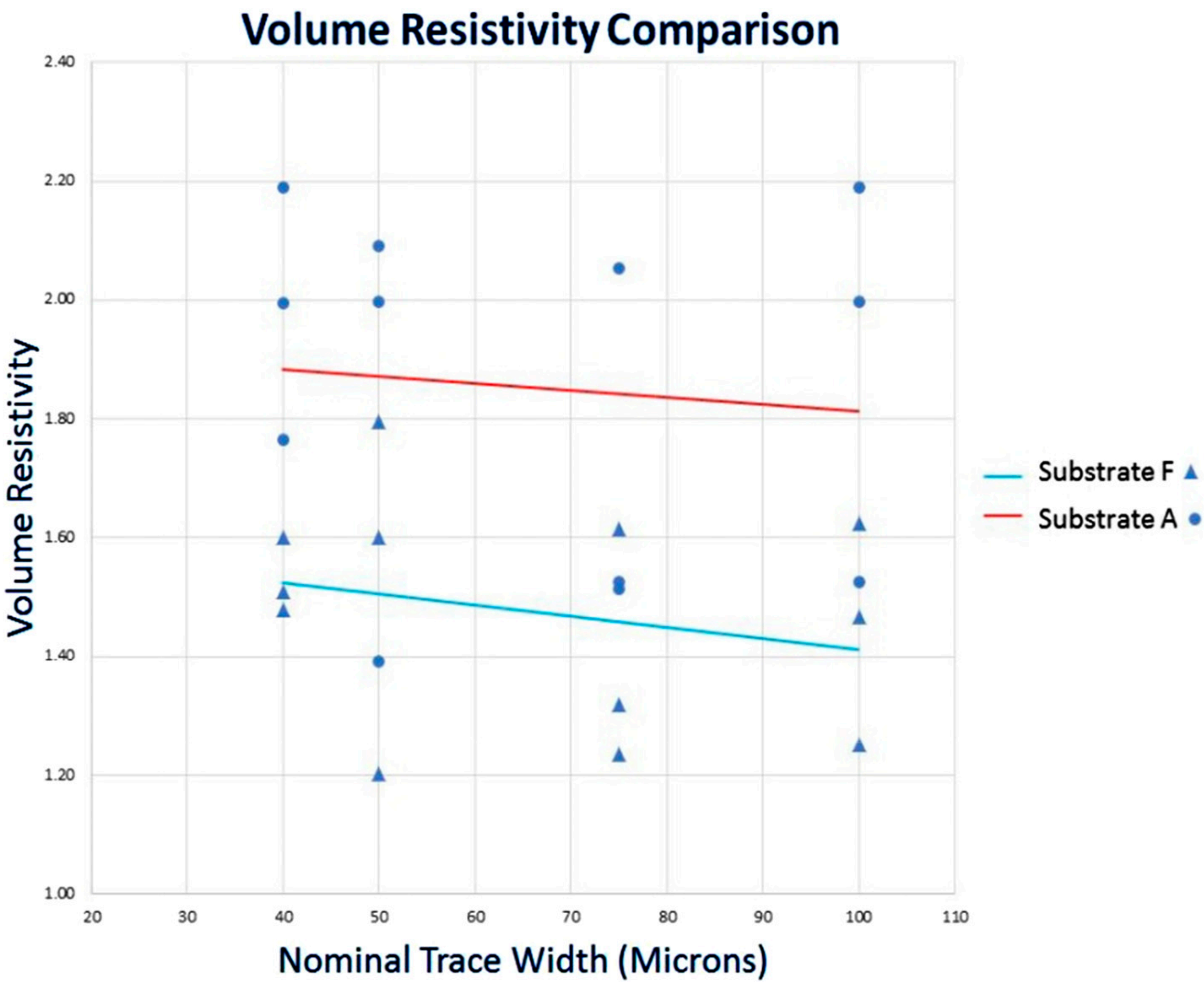


Fig. 28. Volume resistivity data for substrates A and F.

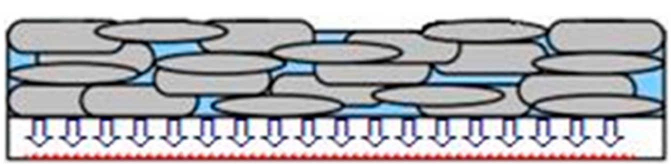

Fig. 29. Depiction of tighter conductive particle packing in paste printed on substrate F due to the "draw in" effect of the substrate coating.

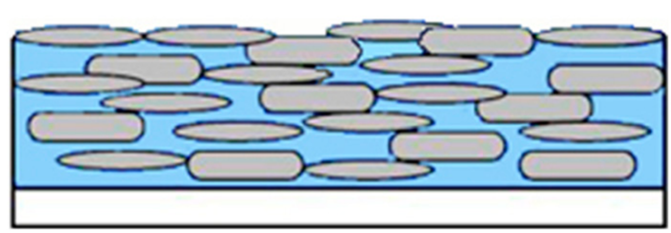

Fig. 30. Depiction of the printed conductive particle dispersion in the paste as it sits on the surface of substrate A or B.

The print test results reported here of the newly developed substrate and emulsion compared with the industry standard PET substrates suggest the intention of the development of these new electronic screen printing–related materials has been realized.

Test results provided in this article show a significant increase in conductivity (14-45%) for the same volume of the same conductive paste when printed on substrate F. This is theorized to be because of the more accurate and consistent 3D profile of conductive traces when printed on substrate F, resulting in tighter packing of conductive particles when the fluids in the paste are drawn into the substrate's surface coating. This increase in printed conductivity seen with substrate F also creates the opportunity to achieve the same level of conductivity currently achieved on substrate A by printing a calculated lesser amount of the same paste, or by printing the same volume of a less conductive paste on substrate F. Either of these scenarios creates the possibility of material cost savings.

## Possible Medical-Related Applications

Possible medical-related applications for the coated substrate would be as follows [3].

As a substrate for circuit elements and components in the following:

1. X-ray equipment
2. Instrument panels
3. Hearing aids
4. Heart pacemakers
5. Medical tool speed controls

Force Sensing Resistors

1. Surgery robotics: patient detect or grip sensing
2. Infusion pumps: to detect block lines and empty bags
3. Patient turning/detection (in/out of bed) sensors
4. Wound care sensors

As interconnect in the following:

1. Defibrillators
2. Ultrasound probe heads
3. Medical pumps
4. STEM/TENS electrode arrays

## Acknowledgments

The author thanks the involved Chromaline/IKONICS team members and industry allies for their expertise, scientific discussion, resources, and materials relating to the testing and analyses of the data presented in this article.

## References

[1] Private discussion with Daniel Kamben, lead chemist, Ikonics Corporation, Duluth, MN.
[2] Private discussion with John Crumpton, technical support specialist, Dow/Dupont, Wilmington, DE.
[3] Private discussion with Michael Wagner, chief technology officer, Butler Technologies, Butler, PA.
[4] Fig. 24 courtesy of Intrinsiq Materials, Inc.